

A Fractographical Study on Dissimilar Weld Joints of SAF 2205 and Hastelloy C-276

Emrullah Çelikkol^{1}, Mustafa Tümer², Ş. Hakan Atapek¹ and M. Zaim Kerimak³*

¹Kocaeli University, Department of Metallurgical and Materials Engineering, Kocaeli, Turkey

²Kocaeli University, Program of Welding Technology, Kocaeli-Turkey

³Anadolu Casting Co., Kocaeli-Turkey

Abstract. In this study, a dissimilar weld joint between SAF 2205 and Hastelloy C-276 was manufactured by using gas tungsten arc welding and its notched impact fracture behaviour was investigated. Initially, V-type welding mouth was opened and the welding was performed by multi-pass. In welding procedure, ERNiCrMo-3 material used as a filler metal and the heat input was varied between 0.48-1.10 kJ/mm depending on welding parameters. Both welding pool and root zone were protected by an argon atmosphere. Multi notched impact tests were performed at room temperature. Weld metal had an impact toughness value as 92 J and its fracture surface exhibited several oriented cracking paths due to its solidified structure. The impact toughness value was measured as 82 J for heat affected zone of SAF 2205 and its fractograph reflected the coarser and deeper dimples. Heat affected zone of nickel based alloy had the highest impact toughness value as 116 J among the studied joints due to the more plastic deformation capability of nickel having face centered cubic structure, however, its fracture surface under impact loading exhibited several cracks propagating throughout the fusion line having equiaxed dendrites.

1 Introduction

Superalloys and stainless steels are widely used in high temperature environments where a combination of strength and resistance to corrosion is required [1, 2]. Among the superalloys, Hastelloy C-276, a nickel-based superalloy, is commonly used in chemical, petrochemical, aviation and nuclear power plant applications due to their high corrosion resistance and high strength properties at elevated temperatures. The alloying elements like chromium, molybdenum and iron provide high yield strength and high corrosion resistance [3-5]. On the other hand, instead of austenitic and ferritic stainless steels, duplex (DSS) and super duplex ones (DSS) have become more attractive in many applications. The matrix consists of a 50/50 ferrite-austenite balance providing a combination of good strength, high toughness and excellent resistance to local corrosion [6-8].

* Corresponding author: celikkolemullah@gmail.com

In mentioned industries, the demand for dissimilar weld joints between Ni-based superalloys and stainless steels has increased. However, compared to Ni-based alloys, the operating temperature of duplex stainless steels (or super duplex stainless steels) is relatively low (up to about 300 °C) due to precipitation of several secondary phases i.e chromium nitrides, chi and sigma. For this reason, Hastelloy C-276 alloy and SAF 2205 dissimilar welding joints are used in the transition from high temperature sections to medium high temperature environments [9, 10]. In this study, initially, a metallurgical analysis of dissimilar weld joints of SAF 2205 and Hastelloy C-276 was done and then notched impact fracture behaviour of the joints were investigated throughout their microstructural features.

2 Experimental study

In this study, SAF 2205 alloy (0.03C-1.34Mn-0.35Si-22.0Cr-5.64Ni-3.22Mo-0.03Nb-0.06V-0.05W, wt.-%) and Hastelloy C-276 alloy (0.002C-15.70Cr-16.20Mo-5.12Fe-0.39Mn-0.002Si-0.14Co-3.74W-0.02V-0.21Al, wt.-%) having dimensions of 5 mm × 10 mm × 55 mm were used as base metals. V-type welding mouth was opened and the welding was performed by gas tungsten arc welding with multi-passes. ERNiCrMo-3 material, a nickel based alloy, was used as the filler metal. The heat input was varied between 0.48-1.10 kJ/mm depending on welding parameters. Both welding pool and root zone were protected by an argon atmosphere.

After welding, the samples taken were mechanically grounded and then polished using alumina powder (3 and 1 µm). The weld metal is electrolytically etched by % 10 oxalic acid for 20 seconds. Both macro and microstructure of the welded parts were characterized and Figure 1 shows a macrostructure of dissimilar joint of SAF 2205 and Hastelloy C-276. In mechanical characterization, multiple notch impact tests were performed at room temperature. The obtained results are shown in Figure 2. SAF 2205 alloy had a higher absorbed energy under notch test compared to nickel based alloy. Solidified weld alloy had the lowest energy level and absorbed energy values of HAZ regions sharply decreased. After the impact test, the fractured parts were examined using a scanning electron microscope (SEM, Jeol JSM 6060).

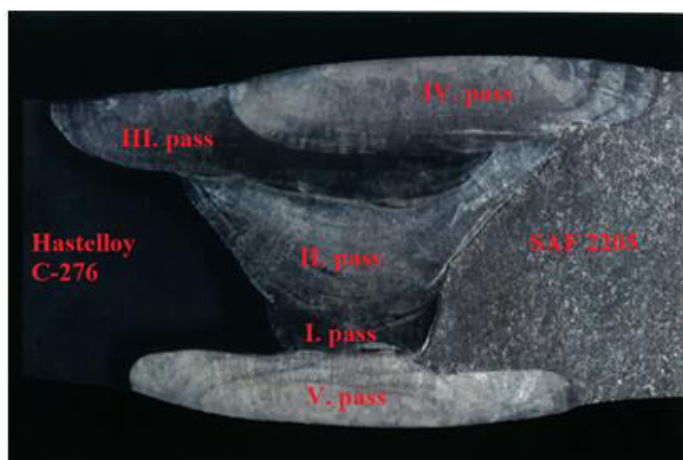


Fig. 1. A macro image showing the dissimilar weld joints of SAF 2205 and Hastelloy C-276.

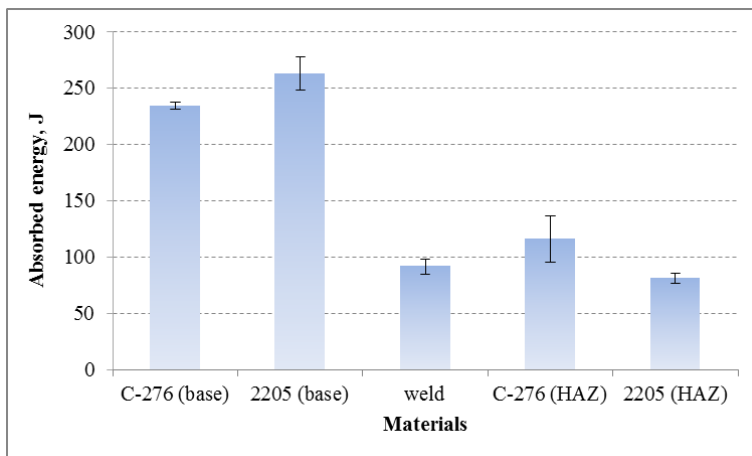


Fig. 2. Obtained absorbed energy values of the materials tested by Charpy V notch impact test.

3 Results and discussion

3.1. Microstructural characterization

Figure 3 shows the microstructures of base alloys; (i) Ni-rich solid solution matrix having a face centered cubic crystal and several twins (Figure 3a) and (ii) a mixture of austenite and ferrite phases (Figure 3b). The fusion zone of welded parts was characterized into three regions according to passes (root, middle and face). In these regions, oriented/equiaxed dendritic and columnar structures were observed depending on the cooling rate within the solidified alloy (Figure 4). In general observations, (i) oriented dendrites and columnar structure were observed within the root part of weld joints and (ii) equiaxed dendrites were observed within the face part of weld.

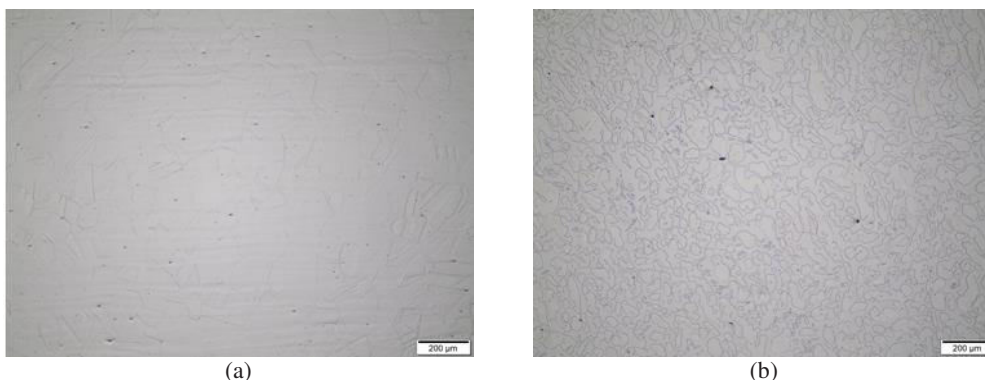


Fig. 3. Microstructures of the studied base alloys; (a) Hastelloy C-276 and (b) SAF 2205.

The base metal structure was changed into heat affected zone and the micrographs given in Figure 5 show the variation of microstructural features. Not only the fraction and also morphologies of austenite and ferrite was changed within HAZ of SAF 2205 alloy (Figure 5a). A coarser grain structure and unmixed zone were observed in the region of HAZ of

Hastelloy C-276 alloy (Figure 5b). As seen in Figure 2, absorbed energies of both stainless steel and nickel based alloy under impact loading are very close; however, the obtained data for HAZs are very low compared to the base alloys. This can be attributed to the variation of microstructural features (i.e fraction of austenite/ferrite, morphology of grain coarsening etc.)

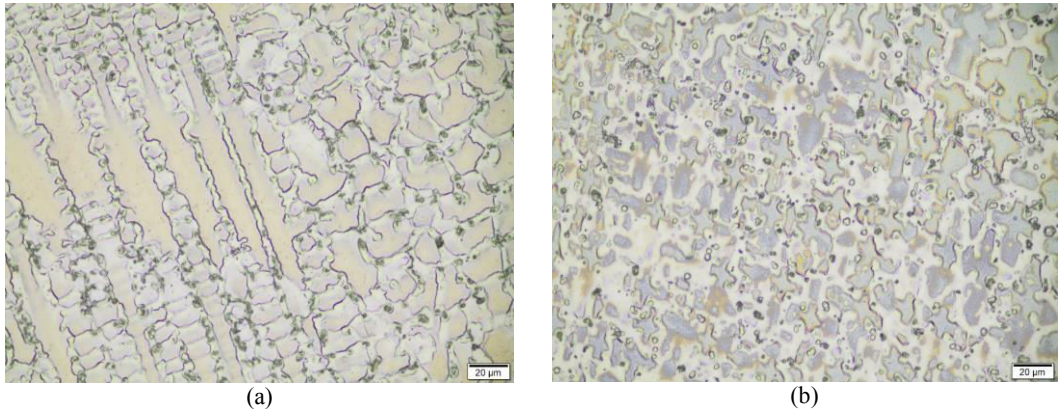


Fig. 4. Oriented dendrites and columnar structure in root pass (a) and equiaxed dendrites in face pass of weld material (b).

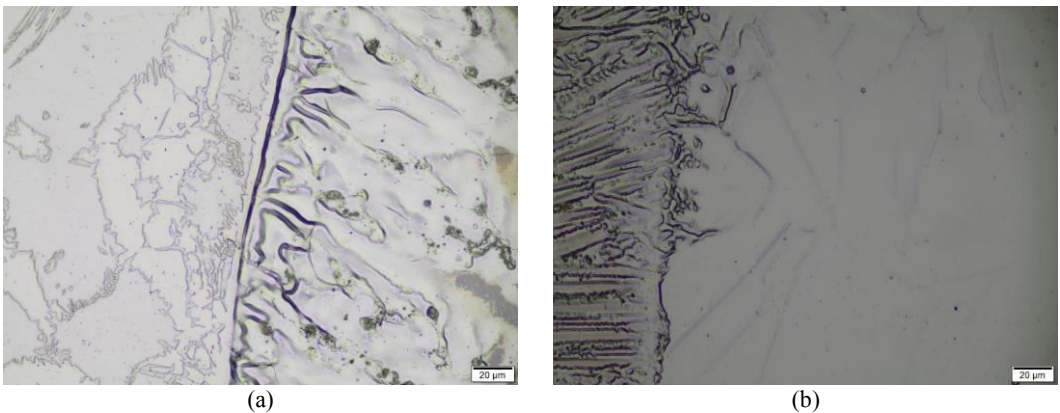


Fig. 5. Variation of microstructural features within the HAZ of SAF 2205 (a) and Hastelloy C-276 alloy (b).

3.2. Fractographical examinations

Impact fracture surfaces of the weld joints were studied by SEM in detail and their cross-sections were characterized in order to reveal out the effect of metallurgical phoneme on the both crack nucleation and propagation. SEM fractographs given in Figure 6 shows the fracture surfaces of weld metal and the fracture surface exhibited typical oriented dimple rupture (Figure 6a). The examinations at higher magnification indicated that several precipitates within the dimples acted as blocker for local plastic glide under impact loading (Figure 6b). The cross-sectional investigations of the weld metal showed the cracks preferably propagated throughout the oriented dendrites (Figure 7).

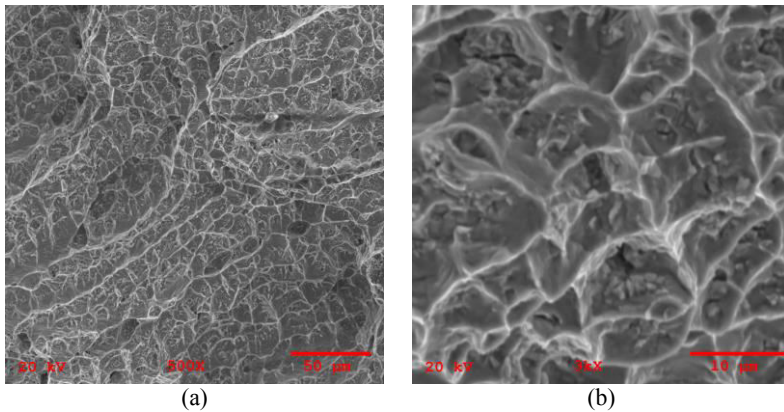


Fig. 6. SEM fractographs showing the impact fracture surface of weld metal (a) and several precipitates within the dimples (b).



Fig. 7. Crack propagation throughout the oriented dendritic structure within the weld metal.

Although the fracture surface of HAZ of SAF 2205 alloy exhibited dimple rupture having plastic deformation capability under impact loading, the fracture surface had coarser dimples compared to those of weld metal (Figure 8a and b). The cracks preferably propagated throughout the fusion line having equiaxed dendrites (Figure 9).

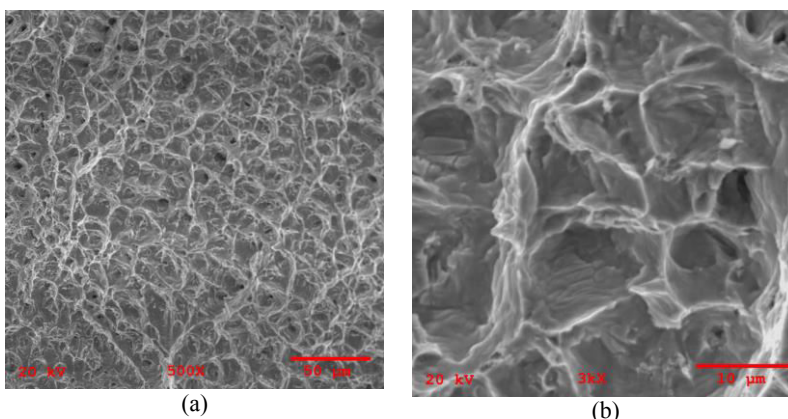


Fig. 8. SEM fractographs showing the impact fracture surface of HAZ of SAF 2205 alloy (a) and coarser dimples (b).

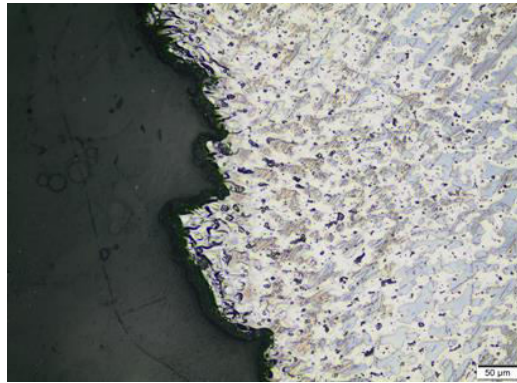


Fig. 9. Crack propagation throughout the equiaxed dendrites within the HAZ of SAF 2205 alloy.

The fracture surface of HAZ of Hastelloy C-276 was also studied and obtained fractographs were given in Figure 10. Its general fracture surface exhibited ductile rupture (Figure 10a), both SEM fractograph (Figure 10b) and cross-sectional image (Figure 11) showed that interdendritic regions formed due to segregation had an important role on the crack nucleation and propagation under impact loading.

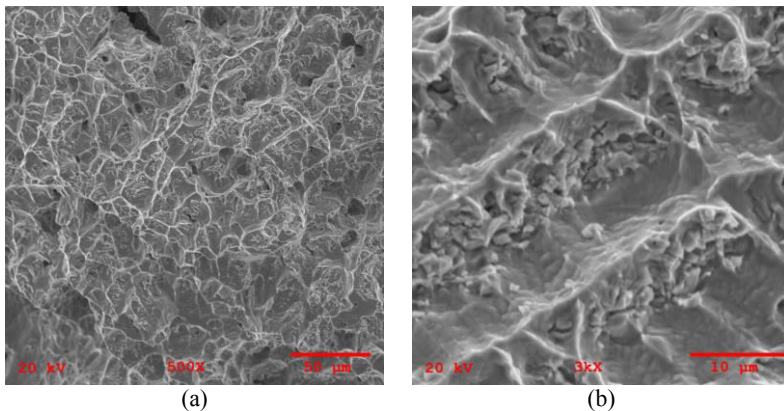


Fig. 10. SEM fractographs showing the impact fracture surface of HAZ of Hastelloy C-276 alloy (a) and crack propagation throughout the interdendrites (b).

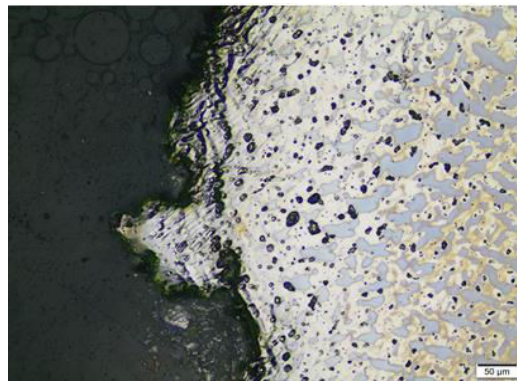


Fig. 11. Crack propagation throughout the equiaxed dendrites within the HAZ of Hastelloy C-276 alloy.

4 Conclusions

In this study, both microstructural and mechanical characterization of a dissimilar weld joint between SAF 2205 and Hastelloy C-276 was investigated and following results were obtained;

(i) weld metal had several morphologies of solidified structure depending on passes having different cooling rate. In root, weld metal exhibited typical oriented dendrites and columnar structure, however, in face, solidified structure consisted of equiaxed dendrites.

(ii) notch impact tests revealed out that both base metals having plastic deformation capability due to their phase characteristics had higher impact toughness value compared to rapidly solidified weld metal and a sharp decrease of toughness was obtained for HAZs due to unmixed zone and coarser grains.

(iii) fractographical examinations showed that fracture surface of weld metal exhibited several oriented cracking paths, coarser and deeper dimples were observed in the fracture surface of HAZ of SAF 2205 and HAZ of Hastelloy C-276 failed by crack propagation throughout the fusion line having equiaxed dendrites.

References

1. K. D. Ramkumar, S. D. Patel, S. S. Praveen, D. J. Choudhury, P. Prabakaran, N. Arivazhagan, M. A. Xavier, *Mater. Design* **62**, 175 (2014)
2. K. D. Ramkumar, P. S. G. Kumar, V.R. Krishna, A. Chandrasekhar, S. Dev, W. S. Abraham, S. Prabhakaran, S. Kalainathan, R. Sridhar, *Mater. Sci. Eng. A* **676**, 88 (2016)
3. S. Sharma, R. V. Taiwade, H. Vashishtha, *JMEP* **26**, 1146 (2017)
4. S. Sharma, R. V. Taiwade, H. Vashishtha, S. Mukherjee, S. Tiwari, *J. Manuf. Process.* **32**, 32 (2018)
5. S. Sharma, R. V. Taiwade, H. Vashishtha, *ISIJ Int.* **57**, 1080 (2017)
6. T. F. A. Santos, H. S. Idagawa, A. J. Ramirez, *Sci. Technol. Weld Joi.* **19**, 150 (2014)
7. A. Motesshaker, I. Danaee, *J. Mater. Sci. & Technol.* **32**, 282 (2016)
8. R. Badji, M. Bouabdallah, B. Bacroix, C. Kahloun, B. Belkessa, H. Maza, *Mater. Charact.* **59**, 447 (2008)
9. J. Kangazian, M. Shamanian, A. Ashrafi, *J. Manuf. Process.* **29**, 376 (2017)
10. J. Kangazian, M. Shamanian, *J. Manuf. Process.* **26**, 407 (2017)